# Receiver Structures for Underwater Acoustical Communications Using Chirp Slope Keying

Edit J. Kaminsky and Madalina Barbu
Department of Electrical Engineering, University of New Orleans, New Orleans, LA, U.S.A.

## ABSTRACT

This paper presents several receiver structures for Chirp Slope Keying (CSK), a digital broadband modulation scheme we propose to use for underwater acoustical communications. In its simplest form, the binary information modulates the slope of a linear chirp, with up-chirps representing ones and down-chirps representing zeros. A time-domain receiver and a novel time-frequency receiver structure based on the Wigner distribution and the Radon Transform are discussed and evaluated in terms of the probability of error versus Signal-to-Noise (SNR) performance. Simulation results and plots are presented for the Additive White Gaussian Noise (AWGN) channel. Results show that if the detector at the receiver operates directly on the slope of the received signal, performance is improved at the expense of computational complexity.

## 1 Introduction

This paper presents receiver structures for chirp slope keying (CSK) a digital spread spectrum communications system we propose to use for acoustical underwater communications. The two receivers discussed are the standard correlation receiver implemented in the time-domain with and integrate and dump device, and a receiver based on time-frequency methods. In the simplest form of CSK, the digital modulating data are represented by the slope of a linear chirp signal, where an up chirp (i.e., increasing frequency) represents a "1" and a down chirp (decreasing frequency) represents a "0". Higher dimensional constellations are easily obtained by using a larger number of up/down slopes, or communication over several signaling intervals. Due to the wide bandwidth, immunity against various frequency selective impediments may be expected.

CSK, as all spread spectrum systems, utilizes a data modulated signal which has its energy spread over a bandwidth which is much greater than the rate of information being sent. The purpose of the work reported here is to introduce and evaluate time-frequency domain receivers for this modulation method. The receivers discussed compute the Wigner time-frequency distribution of the received signal, and then computes the Radon transform of the resulting image. A peak intensity detector on the resulting image is then used to determine whether the transmitted symbol was an up chirp or a down chirp.

We present an overview of chirp-slope keying and demodulation methods as well as the performance evaluation in AWGN. Performance evaluations over the Rayleigh channels using the standard receiver have shown[1] that CSK performs better than standard PSK for certain ranges of SNR because the fading problem is reduced by using broadband signals. Simulations demonstrated that even with the simplest receiver, CSK offers sturdy

Sensors, and Command, Control, Communications, and Intelligence (C3I) Technologies for Homeland Security and Homeland Defense V, edited by Edward M. Carapezza, Proc. of SPIE Vol. 6201, 620110, (2006)
0277-786X/06/$15 · doi: 10.1117/12.659899

performance in the modeled ocean environment. The scheme is expected to be used for underwater acoustical communications where current transmission rates and performance still have enormous room for improvement.[2]

Establishing communication between two remote underwater sites by using cable connected between a receiver and a transmitter, even if possible, has several disadvantages: it is expensive, maintenance and repair are difficult especially if the communication takes place in the deep water, and the drag from the cable can be a problem if the user is small and mobile. A better way is to use sound propagated through water: the underwater acoustic channel (UWA). However, the UWA channel is an unforgiving wireless communication medium. From a communication perspective, the UWA channel poses many challenges to the realization of reliable, high data rate, and long distance communications.

There are four aspects of the UWA channel that are of primary concern: ambient noise, transmission loss due to geometrical spreading and absorption, reverberation due to multipath, and Doppler spreading due to relative motion. Each must be considered in modeling the appropriate UWA channel[3−5] . Ambient noise is caused by man-made activities, sea life, and waves and influences the signal-to-noise ratio which ultimately constrains the data transmission rate for a given probability error (PE) or decreases accuracy for a given rate. Transmission loss is caused by energy spreading and sound absorption.

The most challenging aspect of the UWA channel is the reverberation due to multipath propagation which contributes to signal fading and causes inter-symbol interference (ISI) in digital communication systems. In the past, this multipath propagation resulted in restricting communication in the UWA channel to noncoherent modulation schemes, and low data rates.[3] Doppler spreading is one implication of relative motion between the transmitter and receiver or by ocean internal factors (such as water motion in the channel).

In the past, underwater acoustic communications have received much attention, mostly by the military, associated with submarines detection. In recent years, the applications of underwater acoustic communications are beginning to shift towards commercial applications. Today, underwater communication systems are employed in various unmanned submersibles (e.g. robots, underwater vehicles (ROV's)) which are replacing divers in a variety of offshore work tasks.

This paper deals primarily with alternate demodulation strategies for Chirp-Slope Keying using time-frequency techniques. The rest of this paper is organized as follows: Section 2 summarizes the chirp slope keying scheme, followed in Section 3 by the description of the simple AWGN channel model. Some background information on time-frequency techniques is presented in Section 4. Demodulation of CSK is discussed in Section 5, where our time-frequency detectors are presented. Performance evaluation and simulation results are given in Section 6. Concluding remarks and suggestions for further work are presented in Section 7. References follow.

## 2 Chirp-Slope Keying

Analog chirp signals or linear frequency modulation signals have been used extensively in radar technology and, more recently, in sonar systems. Chirp modulation is one of the older spread spectrum methods which was developed for radar use in the mid-1940s.[6,7] The basic idea is to transmit long frequency modulated pulses in which the frequency changes continuously in one direction (increasing or decreasing) without reversal for the duration of the pulse. Chirp signals in digital communications were seemingly originally suggested by Winkler in 1962[8] and then abandoned. The idea is to use a pair of linear chirps that have opposite chirp rates for binary signaling because of the chirp signal's high robustness against distortions and different types of interference. Binary chirp signals, or what Berni called linear frequency sweeping (LFS),[9] compared favorably to FSK and PSK in coherent channels. In non-coherent channels LFS was considered less appealing because of the requirement for a phase recovery system. Simulation results that show a considerable improvement (at least 3 dB in the SNR ranges of interest where the probability of error is below $10^{-3}$) in performance when CSK is used instead of BPSK in the Rayleigh fading channel have recently appeared.[1]

The use of chirp modulation for multiple access was first proposed by Cook in 1974.[10] He proposed the use of chirp signals hopping different modulation slopes and different bandwidths for multiple-user applications. El-Khamy extended Cook's approach to improve performance in[11].[14] This suggested technique was motivated by the inherent interference rejection capability of such spread-spectrum systems, especially in circumstances where immunity against Doppler shift and fading due to multipath propagation are important. In 2002, Hengstler extended Cook's and El-Khamy's approach using the new chirp modulation spread spectrum (CMSS).[15] Compared to other spread spectrum systems, Hengstler's new CMSS outperforms the existing chirp modulation technique and BER performance attainable by direct sequence spread spectrum systems. In recent years, more authors have researched and utilized chirp signals in communications systems. A chirp FSK modem with 56 narrowband chirp FSK pulses for high reliability communications in shallow water has been discussed.[16,17] Experiments showed that the system is virtually insensitive to selective fading, reverberation, and Doppler.

In this paper, simple linear-up and linear-down chirp signals are used to represent binary 0 and 1, respectively. A linear complex chirp signal may be modeled as:

$$S_c(t) = A\exp\left[j(\omega_0 t + \beta t^2)\right] = A\exp\left[j\pi\left(2f_0 t + \mu_0 t^2\right)\right] \tag{1}$$

where $\omega_0$ is the carrier angular frequency and $\beta$ is the chirp rate. The real part of 1 is used as the transmitted signal, with the slope indicating the transmitted bit:

$$S(t) = \mathrm{Re}\left\{S_c(t)\right\} = A\cos\left[2\pi\left(f_0 t + \frac{\mu_0}{2}t^2\right)\right] \tag{2}$$

The instantaneous frequency, then, is given by

$$\frac{1}{2\pi}\frac{d\varphi(t)}{dt} = f_0 + \mu_0 t \tag{3}$$

In terms of maximum and minimum instantaneous frequencies, $f_{\max}$ and $f_{\min}$, an up chirp is represented as in (4), while a down chirp is represented by (5).

$$S_u(t) = A\cos\left[2\pi t\left(f_{\min} + \frac{f_{\max} - f_{\min}}{2T}t\right)\right] \tag{4}$$

$$S_d(t) = A\cos\left[2\pi t\left(f_{\max} - \frac{f_{\max} - f_{\min}}{2T}t\right)\right] \tag{5}$$

The CSK scheme, then, works as follows: the binary stream $\{B_i\}$ selects the chirp pulses $\{p_i(t)\}$ to be transmitted at each signalling interval based on its value:

$$p_i(t) = \begin{cases} S_u(t), & B_i = 1 \\ S_d(t), & B_i = 0 \end{cases} \tag{6}$$

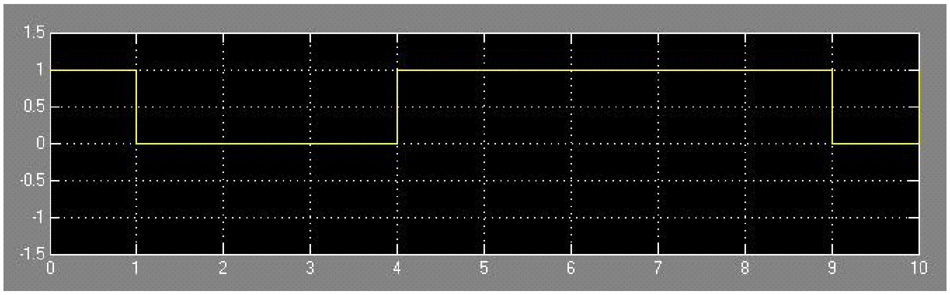


Figure 1: Binary message to be transmitted.

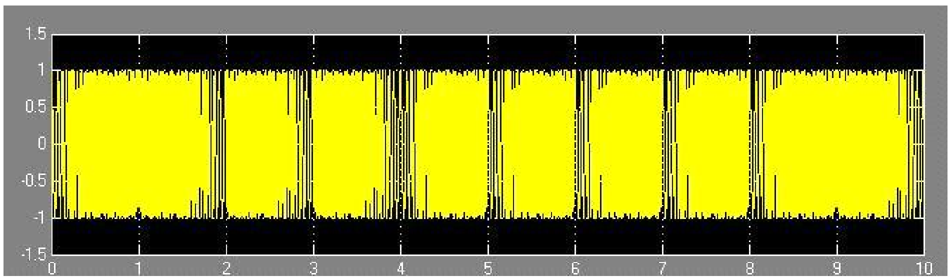


Figure 2: Sequence of transmitted up and down chirps corresponding to the binary sequence above.

A typical binary sequence and the transmitted waveform are sown in Fig. 1 and 2, respectively.

# 3 AWGN Channel Model

Because the current contribution is the presentation and evaluation of time-frequency receivers for CSK, a very simple model will be used to simulate the UWA channel's ambient noise in this paper: the additive white Gaussian noise (AWGN) channel. Many researchers use the Additive White Gaussian Noise (AWGN) to model the ambient noise in underwater channels[18]-.[19–22]

If the signal s(t) is transmitted through the underwater channel, the received signal r(t) can be modeled as:

$$r(t) = A_r\,[s(t) + n(t)] \tag{7}$$

where $A_r$ is some scaling constant, $n(t)$ is the zero-mean stationary Gaussian random process. We define signal-to-noise ration (SNR) as

$$\text{SNR }(dB) = 10\log_{10}\frac{E_s}{E_n} \tag{8}$$

with $E_s$ as the signal energy in one symbol $s(t)$ and $E_n$ is the double sided power of the white Gaussian noise process, given respectively as:

$$E_s = \frac{1}{T}\int_{-T/2}^{T/2} \cos^2\left[2\pi\left(f_0 t + \frac{\mu_0}{2}t^2\right)\right] dt \tag{9}$$

$$E_n = 2W\sigma_g^2 \tag{10}$$

where $W$ is defined as the channel bandwidth and $\sigma_g^2$ is the variance of the AWGN. Equation (9) yields Fresnel integrals; with the assumption that the arguments of $\mathrm{C}_f(\mathrm{x})$ and $\mathrm{S}_f(\mathrm{x})$ are large numbers, $\mathrm{C}_f(\mathrm{x})$ and $\mathrm{S}_f(\mathrm{x})$ approach 1/2, so that the power of the linear chirp can be well approximated to be just above 1/2.

# 4 Wigner Distribution and the Radon Transform

Our receiver works on the time-frequency domain where a chirp is a straight line (with a positive slope for a transmitted "1" and a negative slope for a transmitted "0"). This section summarizes relevant techniques.

## 4.1 The Wigner Distribution

Numerous time-frequency distributions have been proposed over the years. Efforts have also focused in increasing the localization of the signal components in the time-frequency (t-f) plane. A pleasantly well written and easy to understand review was authored by Cohen,[23] where fundamental ideas and methods, as well as discussion of the most frequently used time-frequency distributions is presented. The common goal of all distributions is to represent the energy or intensity of a signal simultaneously in time and frequency showing how the spectral content of the signal changes with time. Although myriad different distributions, each with its own pros and cons, are available for analysis, we shall concentrate on the Wigner (or Wigner-Ville[1], WVD) distribution.

The Wigner distribution has a product kernel, satisfies the marginals, is real, and time and frequency shifts in the signal produce corresponding time and frequency shifts in the distribution. This distribution reduces the interference terms at the expense of opposed time and frequency resolutions. The Wigner distribution is positive only for Gaussian signals. The Wigner distribution (WD) provides a powerful theoretical basis for quadratic time-frequency analysis and its discrete form is an important tool in signal analysis. The WD can be given in terms of the signal $s(t)$ or in terms of the spectrum

$$S(\omega) : W(t,\omega) = \frac{1}{2\pi}\int_{-\infty}^{\infty} s^*(t-\frac{1}{2}\tau)s(t+\frac{1}{2}\tau)e^{-j\tau\omega}d\tau = \frac{1}{2\pi}\int_{-\infty}^{\infty} S^*(\omega-\frac{1}{2}\theta)S(\omega+\frac{1}{2}\theta)e^{-jt\theta}d\theta \tag{11}$$

In terms of frequency $f$, the Wigner-Ville distribution (WVD), $W_z$, of the analytical signal $z(t)$ is given by:

$$W_z(t,f) = \int_{-\infty}^{\infty} z(t+\tau/2)\ z^*(t-\tau/2)\ e^{-j2\pi f\tau}d\tau \tag{12}$$

[1] Ville used the characteristic function method to derive the Wigner distribution.

According to[23] it was Martin who coined the phrase "Wigner-Ville spectrum" to indicate the Wigner distribution that has been averaged over an ensemble of possible realizations of the signal. WD is said to be bilinear because the signal enters twice in the calculation.

### 4.2 Radon Transform

The Radon transform is a commonly used technique to detect straight lines in image data. The transform requires that the desired features be specified in some parametric form. We wish to find straight lines (the slope of the chirp in frequency vs time) so we assume them parameterized in the form $x \cos\theta + y \sin\theta = r$, where $r$ is the perpendicular distance from the origin and $\theta$ is the angle with the normal. Collinear points $(x_i, y_i)$, with $i = 1, \ldots, N$, are transformed into N sinusoidal curves in the $(r, \theta)$ plane. Or, said in the opposite way, for any point on a line, $r$ and $\theta$ are constant. The Radon transform may be used to implement the straight-line detection implementation of the Hough transform; this is what we do.

The Radon transform is the projection of the image intensity along a radial line oriented at a specific angle. The Radon transform for a set of parameters $(r, \theta)$ is the line integral through the image g(x,y), where the line is positioned corresponding to the value of $(r, \theta)$:

$$g(r, \theta) = \int_{-\infty}^{\infty} g(r \cos\theta - s \sin\theta, r \sin\theta + s \cos\theta) \; ds \tag{13}$$

or, equivalently

$$g(r, \theta) = \int_{-\infty}^{\infty} \int_{-\infty}^{\infty} g(x, y) \delta(x \cos\theta + y \sin\theta - r) \; dx dy \tag{14}$$

Figure 3 depicts the image that results from taking the Wigner distribution of a down chirp signal with AWGN of variance 0.4 (SNR = 25 dB). Clearly, the Wigner distribution of the chirp function is found to be concentrated along the line giving the instantaneous frequency of the chirp. The Radon transform of this signal is depicted in Fig. 4, where we see that a down chirp of the characteristics used produces a peak in the Radon transform at an angle $\theta$ of 80 degrees. The position of the bright spot depends on the characteristics of the chirp and it can be used for determining if the chirp's slop is positive or negative. The characteristics of the chirps used in our simulations are given in Table 1.

When the noise is increased to have a variance of 1 (SNR = 21 dB) and is added to an up chirp, the resulting Wigner distribution is shown in Fig. 5. The Radon transform for this case is given in Fig. 6, which still shows that the peak is clearly identifiable; for up chirps of the characteristics used, the peak occurs at $\theta$ of 102 degrees. The radial coordinates returned are the values along the x′ axis, which is oriented at $\theta$ degrees counterclockwise from the x-axis.

Table 1: CSK simulation parameters

| Parameter | Value |
|---|---|
| Symbol rate | 1 s |
| Sampling rate | 512 samples/s |
| $f_{min}$ | 25 Hz |
| $f_{max}$ | 125 Hz |
| Chirp rate (slope) | 100 Hz/s |

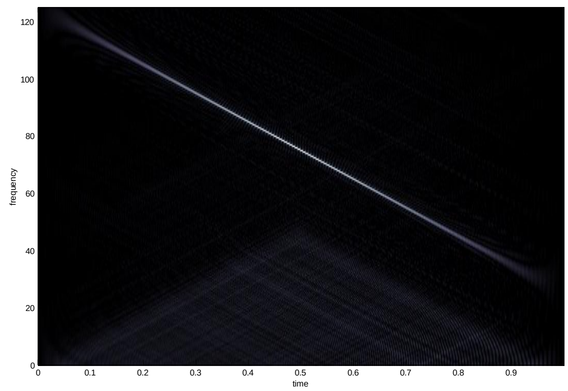


Figure 3: Wigner distribution of a down chirp with little noise (variance of 0.4.)

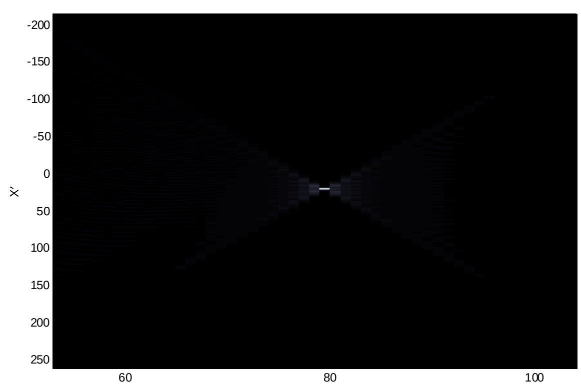


Figure 4: Radon transform of the Wigner distribution of a down chirp with little noise.

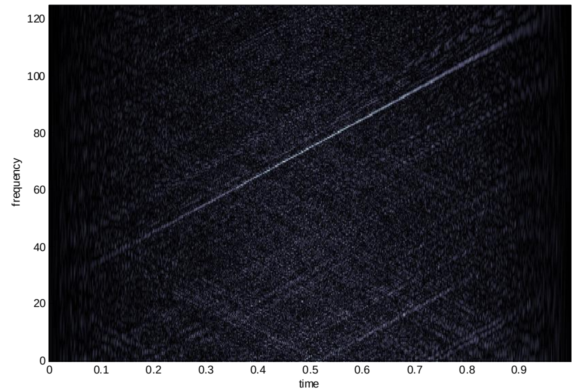


Figure 5: Wigner distribution of up chirp with AWGN of variance 1.

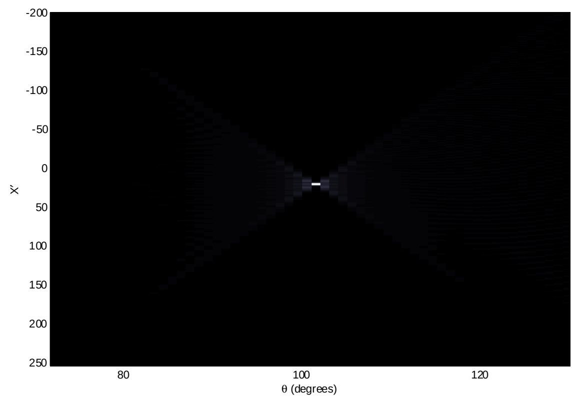


Figure 6: Radon transform of the Wigner distributuion of the up chirp with AWGN of variance 1.

# 5 CSK Receivers

Analysis of Figs. 4 and 6 gives us an idea of how to proceed with a time-frequency detector. We first must compute the appropriate transformation into the time-frequency domain –i.e., the Wigner distribution– and take the Radon transform of the resulting image. The Radon transform will have its brightest spot at $\theta = 80^\circ$ if the signal transmitted was a down chirp and at $\theta = 102^\circ$ if the transmitted signal is an up chirp, corresponding to a logic 1. A threshold in the middle, i.e. at $\theta_t = 91^\circ$ will be able to separate up chirps from down chirps in the Radon space. Clearly we can first window the images to make computations faster and computer use more efficient. In our work, we only compute the Radon transform for angles in the ranges $77^\circ \leq \theta \leq 83^\circ$ and $99^\circ \leq \theta \leq 105^\circ$, i.e., $3^\circ$ on either side of the ideal values.

The two receivers that we're comparing are shown in schematic form in Figures 7 and 8, for the correlation-type receiver[1] and the time-frequency receiver discussed here, respectively.

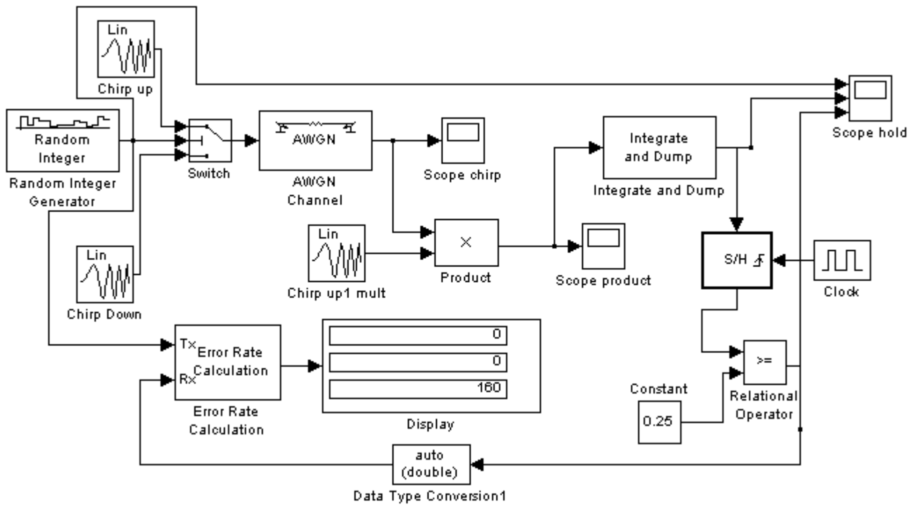


Figure 7: Simulink implementation of the time-domain detector for binary CSK.

A random binary number generator block creates equally likely binary digits which in turn select, through the switch, the type of chirp transmitted through the AWGN channel. The chirp signal generator blocks generate the linear up and down chirp signals. The integrate-and-dump block in Fig. 7 integrates the input signal in discrete time and resets to zero every period T. The sample-and-hold block acquires $y(t)$ whenever it receives a trigger from the clock and holds the value for a whole period. Because the output of the sample-and-hold block has to wait for a whole period, the demodulated data is delayed by T. The "Matlab function" block in Fig. 8 is a short Matlab mfile that implements the Wigner distribution computation and the Radon transform of a windowed version of the result. The parameters used in the simulations are those given before in Table 1.

# 6 Results

Performance evaluation of CSK was performed for the AWGN channel using the time-domain and the time-frequency domain receivers. Due to the added computational complexity, the time-frequency receiver simulations ran much more slowly than the time-domain receiver. The simulated BER curves were obtained by computing the probability of error after at least 10 bits errors, for each SNR value.

Fig 9 shows the bit error rate versus the signal to noise ratio graphs of the CSK in this channel for both receiver implementations: time-domain (correlation-type) receiver, and the time-frequency domain (Wigner-Radon) receiver. The two receivers' performance cross at around 15 dB. For SNR smaller than 15 dB, the performance of the time-domain receiver is better while for SNR larger than about 15 dB the performance is best for the time-frequency receiver. Notice, however that the cases of interest are usually for low probability of error and these are the ranges for which the time-frequency receiver performs better.

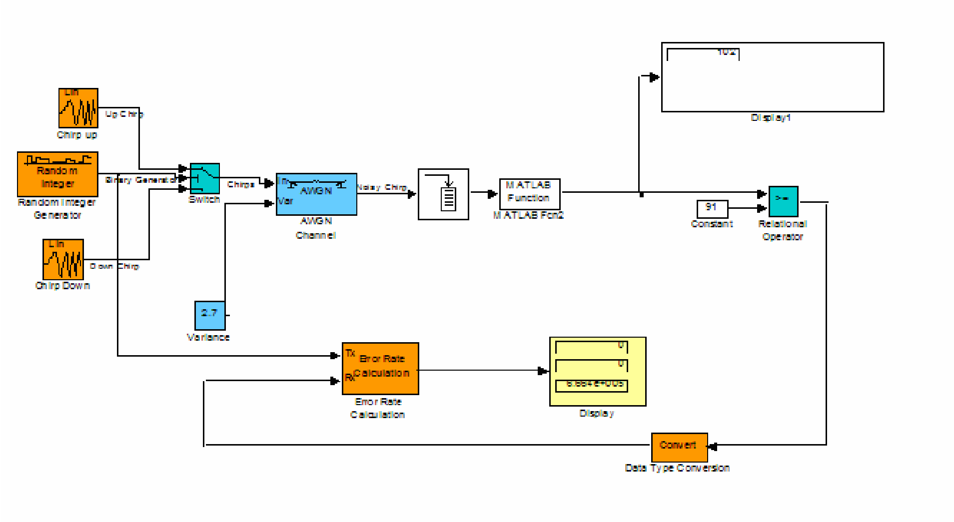


Figure 8: Simulated time-frequency receiver for CSK.

## 7 Conclusions and Suggestions for Further Work

We have presented a discussion of two receivers for a digital modulation method using Chirp Slope Keying (CSK) for underwater acoustic communications. By implementing an integrate-and-dump product receiver, we showed good quality of detection of the transmitted binary signal; this receiver's implementation is straightforward, of low computational complexity, and fast. The second receiver tries to detect the slope of the chirp directly in the time-frequency plane. This is done by first computing the Wigner distribution of the received signal, which converts the time-domain noisy chirp into a time-frequency image. The Radon transform is then used to determine where a straight line is present in the t-f domain. We know, a priori, that the angle $\theta$ determines whether the found lines have positive or negative slopes. A threshold in the middle is used to finally detect the chirp as up-chirp or down-chirp.

The channel model simulated was simply the additive white Gaussian noise (AWGN) channel. A better model for the underwater acoustic channel would be a Rayleigh fading channel with multipath signals with shifts in time, phase, and frequency (Doppler). Performance evaluation in those more realistic channels must be done.

The performance of any communication system is heavily dependent on the internal and external synchronizations. For the time-based receiver we assumed that both synchronizations were achieved without error; this assumption is not very realistic. The time-frequency receiver, however, does not rely so heavily on these assumptions –time synchrony will be needed, but not phase coherence– and is therefore expected to perform much better than the time-domain receiver when synchronization problems occur. Another possible future research area would concentrate on determining the degradation of the system performance due to synchronization errors.

A larger improvement of binary CSK over standard modulation schemes is expected as channel conditions deteriorate. PSK is very sensitive to phase shift and Rayleigh amplitude. FSK is extremely sensitive to frequency shift and frequency selective fading. ASK cannot handle amplitude fading. Even though CSK's performance is worse than BPSK in the benign AWGN channel, this deficit decreases as channel conditions worsen. Evaluation of our CSK receivers in these very deleterious channels should be done.

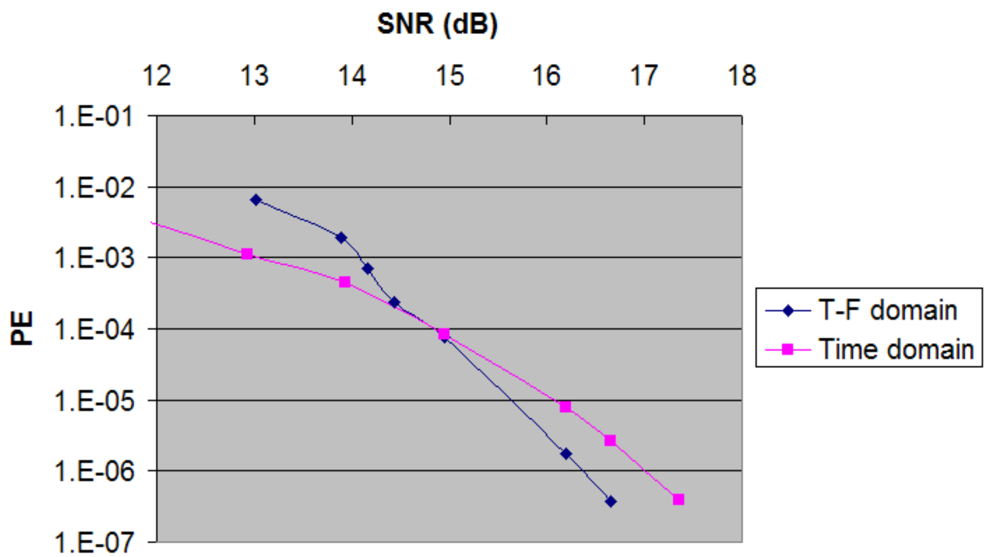


Figure 9: Probability of bit error vs SNR in dB for the time-domain and the time-frequency domain receivers.

## 8 REFERENCES


[1] Edit J. Kaminsky and Lastri Simanjuntak, "Chirp slope keying for underwater communications," in *Proc. SPIE Vol. 5778, Conf. On Sensors, and Command, Control, Communications, and Intelligence (C31) Technologies for Homeland Security and Homeland Defense IV*, Orlando, FL, April 2005, pp. 894–905, SPIE.

[2] D. B. Kilfoyle, James C. Preisig, and Milica Stojanovic, "Special issue on underwater acoustic communications," *IEEE Transactions on Oceanic Engineering*, vol. 25, no. 1, January 2000.

[3] M. Stojanovic, "Underwater acoustic communications," *IEEE Electro International*, pp. 435–440, June 1995.

[4] W. S. Burdic, *Underwater Acoustic System Analysis*, Prentice Hall, 1991.

[5] A. B. Baggeroer, "Acoustic telemetry –An overview," *IEEE Journal of Oceaninc Engineering*, vol. OE-9, no. 4, pp. 229–235, October 1984.

[6] J. Holmes, *Encyclopedia of Science and Technology*, vol. 17, chapter Spread Spectrum Communication, pp. 271–273, McGraw-Hill, 8 edition, 1997.

[7] J. R. Klauder, A. C. Price, S. Darlington, and W. J. Albersheim, "The theory and design of chirp radars," *Bell Syst. Tech. Journal*, vol. 39, pp. 745–808, 1960.

[8] M. R. Winkler, "Chirp signals for communications," in *WESCON Convention Record*, 1962, p. Paper 14.2.

[9] A. J. Berni and W. D. Greeg, "On the utility of chirp modulation for digital signaling," *IEEE Transactions on Communications*, vol. 21, no. 6, pp. 748–751, June 1973.

[10] C. E. Cook, "Linear FM signal formats for beacon and communication systems," *IEEE Transactions on Aerospace and Electronic Systems*, vol. AES-10, no. 4, pp. 471–478, July 1974.

[11] S. E. El-Khamy, S. E. Shaaban, and E. A. Thabet, "Partially coherent detection of continuous phase chirp (CPCM) signals," in *Proc. Thirteenth National Radio Science Conference*, March 1996, pp. 485–495.

[12] S. E. El-Khamy, S. E. Shaaban, and E. A. Thabet, "Multi-user chirp modulations signals (M-CM) for efficient multiple-access communication systems," in *Proc. Thirteenth National Radio Science Conference*, March 1996, pp. 289–297.

[13] S. E. El-Khamy, S. E. Shaaban, and E. A. Thabet, "Frequency-hopped multi-user chirp modulation (FH/M-CM) for multiple fading channels," in *Proc. Sixteenth National Radio Science Conference*, 1999, pp. C6/1–C6/8.

[14] S. E. El-Khamy and S. E. Shaaban, "Efficient multiple access communications using multi user chirp modulation signals," in *Proc. 4th IEEE International Symposium on Spread Spectrum Techniques and Applications*. September 1996, vol. 3, pp. 1209–1213, IEEE.

[15] S. Hengstler, D. P. Kasilingam, and A. H. Costa, "A novel chirp modulation spread spectrum technique for multiple access," in *Proceedings of the IEEE International Symposium on Spread Spectrum Techniques and Applications*, September 2002, vol. 1, pp. 73–77.

[16] L. R. Leblanc, P. Beaujean, M. Singer, C. Boubli, and G. T. Strutt, "Chirp FSK modem for high reliability communication in shallow water," in *Proc. Oceans 1999*. September 1999, vol. 1, pp. 222–227, IEEE/MTS.

[17] L. R. Leblanc, M. Singer, P. Beaujean, C. Boubli, and J. R. Alleyne, "Improved chirp FSK modem for high reliability communications in shallow water," in *Proc Oceans 2000*. September 2000, vol. 1, pp. 601–603, MTS/IEEE.

[18] D. B. Kilfoyle and A. B. Baggeroer, "The state of the art in underwater acoustic telemetry," *IEEE Journal of Oceanic Engineering*, vol. 25, no. 1, pp. 4–27, January 2000.

[19] H. V. Poor, "Uncertainty tolerance in underwater acoustic signal processing," *IEEE Journal of Oceanic Engineering*, vol. OE-12, no. 1, pp. 48–65, January 1987.

[20] T. Eggen, A. Baggeroer, and J. Preisig, "Communication over doppler spread channels –Part I: Channel and receiver presentation," *IEEE Journal of Oceanic Engineering*, vol. 25, no. 1, pp. 62–71, January 2000.

[21] T. Eggen, A. Baggeroer, and J. Preisig, "Communication over doppler spread channels –Part II: Receiver characterization and practical results," *IEEE Journal of Oceanic Engineering*, vol. 26, no. 4, pp. 612–621, October 2001.

[22] S. Hengstler, "A novel chirp modulation spread spectrum technique for multiple access," M.S. thesis, University of Massachusetts Dartmouth, 2001.

[23] Leon Cohen, "Time-frequency distributions - a review," *Proc. IEEE*, vol. 77, no. 7, pp. 941–981, July 1989.